OPEN

Correspondence and
requests for materials
should be addressed to
P.X. (pingxu@sjtu.edu.
cn)

* These authors
contributed equally to
this work.

Genomic analysis of *Pseudomonas putida*: genes in a genome island are crucial for nicotine degradation

Hongzhi Tang*, Yuxiang Yao*, Lijuan Wang, Hao Yu, Yiling Ren, Geng Wu & Ping Xu

State Key Laboratory of Microbial Metabolism & School of Life Sciences and Biotechnology, Shanghai Jiao Tong University, Shanghai 200240, PR China.

Nicotine is an important chemical compound in nature that has been regarded as an environmental toxicant causing various preventable diseases. Several bacterial species are adapted to decompose this heterocyclic compound, including *Pseudomonas* and *Arthrobacter*. *Pseudomonas putida* S16 is a bacterium that degrades nicotine through the pyrrolidine pathway, similar to that present in animals. The corresponding late steps of the nicotine degradation pathway in *P. putida* S16 was first proposed and demonstrated to be from 2,5-dihydroxy-pyridine through the intermediates *N*-formylmaleamic acid, maleamic acid, maleic acid, and fumaric acid. Genomics of strain S16 revealed that genes located in the largest genome island play a major role in nicotine degradation and may originate from other strains, as suggested by the constructed phylogenetic tree and the results of comparative genomic analysis. The deletion of gene *hpo* showed that this gene is essential for nicotine degradation. This study defines the mechanism of nicotine degradation.

S ignificant amounts of nicotine wastes are produced by tobacco factories, resulting in various environmental and health effects[1]. Microbial organisms play important roles in the tobacco manufacturing process by altering the content of nicotine[2,3]. Recently, *Pseudomonas* spp. strains were integrated in the processing of tobacco products and the treatment of tobacco wastes[4–11]. The Gram-negative soil bacterium *P. putida* S16 has the ability to degrade nicotine[9]. The basic steps and corresponding intermediates of nicotine catabolism generating 2,5-dihydroxy-pyridine (DHP) were earlier reported by Wada and Xu[6,7,12]. A gene cluster (here designated as *nic*1) containing the genes encoding nicotine oxidoreductase (NicA) and 6-hydroxy-3-succinoylpyridine hydroxylase (HspA) is involved in the catabolism of nicotine to DHP (Fig. 1A) in *P. putida* S16[13,14]. A second HSP hydroxylase (HspB), a more active form than HspA with only 11% amino acid sequence homology, was purified and characterized. The *hspB* gene deletion showed that this gene is essential for nicotine degradation, and site-directed mutagenesis identified an FAD binding domain[15]. However, despite the work described above, our understanding is still incomplete, especially the late steps of nicotine degradation. Recently, the genome sequence of strain S16 was completed[16], and it helps us to further identify the genomic and metabolic diversity of this species (Fig. S1). In addition, a DHP oxidase in nicotinic acid degradation from *P. putida* N-9 was earlier purified and crystallized by Rittenberg and coworkers[17]. Moreover, Jimenez *et al*. identified and characterized a gene cluster (*nic* genes) responsible for the aerobic nicotinic acid degradation in *P. putida* KT2440[18]. The mechanism of DHP transformation may be similar during nicotine degradation and nicotinic acid degradation in *Pseudomonas*. All the above information may be helpful in data mining and identification of related genes in the late steps of nicotine degradation.

This study reports a gene cluster (here designated as *nic*2) encoding for 5 factors that mediate in the conversion of HSP to fumarate, of which the *hspB* gene is included. The late steps of the nicotine degradation pathway in *P. putida* S16 was first proposed to be from DHP through the intermediates, *N*-formylmaleamic acid, maleamic acid and maleic acid, to fumaric acid, as indicated in the red dashed box in Fig. 1A. Four genes, namely 2,5-DHP dioxygenase gene (*hpo*), *N*-formylmaleamate deformylase gene (*nfo*), maleamate amidase gene (*ami*) and maleate *cis-trans* isomerase gene (*iso*) in the *nic*2 cluster from strain S16, were cloned and expressed in *Escherichia coli*, and all the related enzymes were characterized. The objective of this work is to demonstrate the unknown catabolism involved in the late steps of the nicotine degradation pathway.

Results

Identification of a gene cluster encoding the late pathway. The first fragment of a *nic* gene cluster (here designated as *nic*2) catalyzing the late steps of nicotine degradation was identified using in silico analysis of
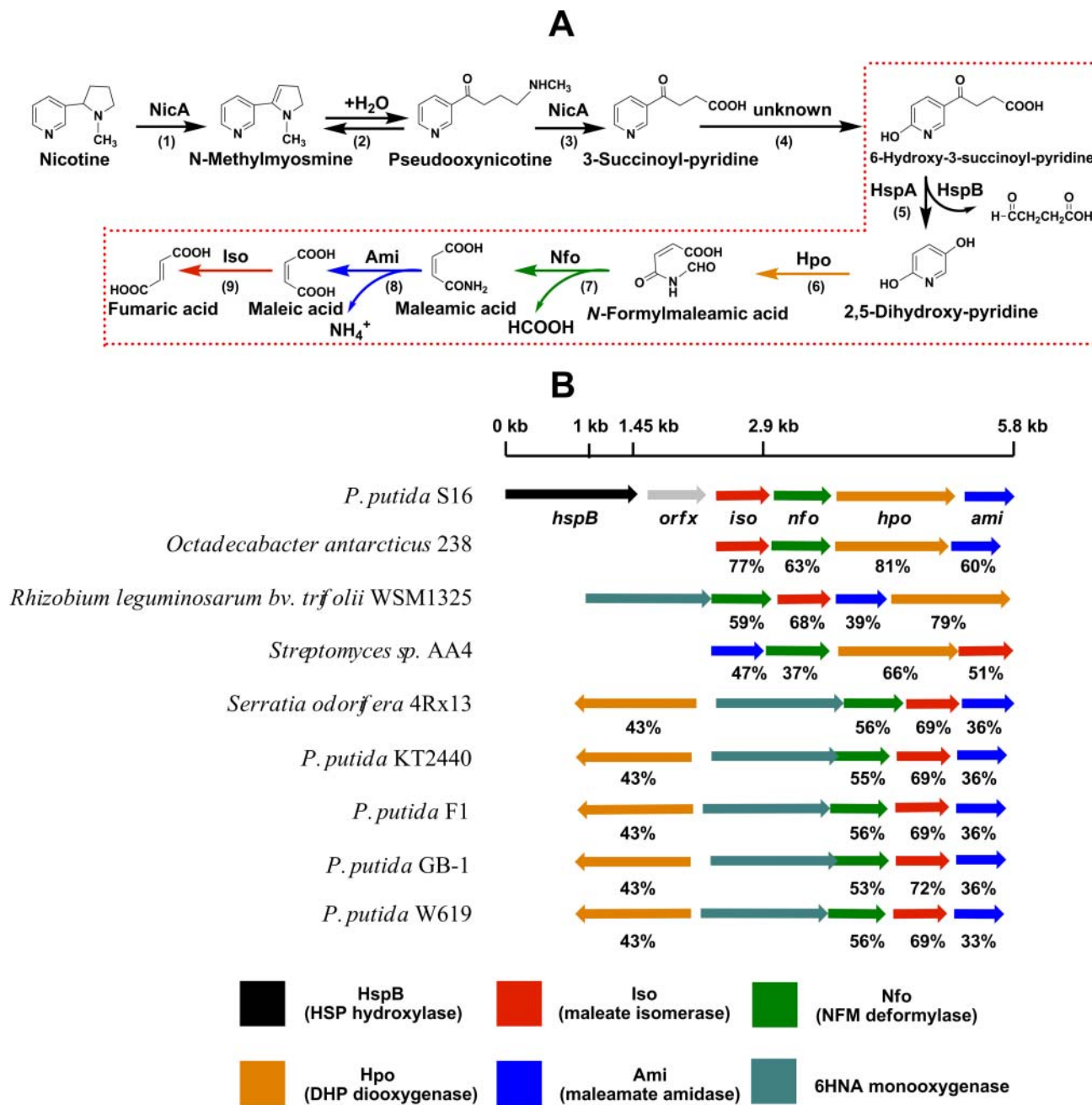
Figure 1 | **Chemical reactions and genes involved in the nicotine degradation pathway of *P. putida* S16.** (A) Pyrrolidine pathway of nicotine degradation. The reactions performed by the enzymes encoded by the *nic*2 gene cluster are inside the red-dashed box. (B) Genetic organization of the *nic*2 cluster of *P. putida* S16 as compared with similar gene clusters from other bacteria. HspB, HSP hydroxylase (black); Iso, maleate isomerase (red); Nfo, NFM deformylase (green); Hpo, DHP dioxygenase (orange); Ami, maleamate amidase (blue); Hna, 6-hydroxynicotinate 3-monooxygenase (dark cyan); Orfx, no predicted function (grey). The percentages represent amino acid homology of related enzymes.

the *P. putida* S16 genome sequence, the *nic* gene cluster in KT2440, and the gene sequence of HspB. The entire 5.8-kb *nic*2 gene cluster was cloned into pMD18T. Resting cells of *E. coli* DH5α containing the pMD18T-*nic*2 construct degraded HSP completely within 9 h at 30°C and 37°C temperatures (data not shown). Fig. 1B shows the chromosomal *nic*2 gene cluster consisting of 6 open reading frames (ORFs). No sequences could be found by BLAST search, using the S16-*nic* cluster (*hspB-ami* part, 5,763 bp, GC content 47.9%) and *nic* cluster (*iso-ami* part, 3,233 bp, GC content 48.0%). The G+C content of the S16-*nic*2 cluster (47.9%) is considerably lower than the average for the *P. putida* S16 genome (62.3%). The 4 downstream enzymes catalyze steps 6-9 of the pathway (DHP to fumaric acid)

(Fig. 1), and have orthologs in other bacteria, some of which are known to degrade nicotinic acid but not nicotine (Fig. 1B). The similarities among these orthologs are as low as 33% (indicated by the fading colors of the ORFs in Fig. 1). The dark cyan arrow indicates a nicotinic acid monooxygenase (6-hydroxy-nicotate 3-monooxygenase, Hna), which has no ortholog in *P. putida* S16. The enzymatic activities of all four proteins of *P. putida* S16 have been verified. The presumptive ATG start codon was detected in *nfo*, *hpo*, and *ami*, whereas the rare initiation codon GTG was found for *iso*. The Shine-Dalgarno sequences[19] were identified in the upstream regions of the putative start codon of *hpo* ('GAGAGGCG-CGATATG'), and that of *ami* ('AAGGAGTATTATATG')[19]. The 4

genes are tightly linked, with no bases between the termination of *iso* and the start of *nfo*, 12 bases between the termination of *nfo* and the start of *hpo*, and 38 bases between the termination of *hpo* and the start of *ami*. Non-quantitative reverse transcription polymerase chain reaction (RT-PCR) showed that the 4 genes appeared to be upregulated in 6 mM nicotine or 1 mM DHP addition separately, whereas no significant effects in the 4 genes expressions were observed with the individual addition of 1 mM NFM, 6 mM maleamic acid, or 6 mM maleic acid (Fig. S2A and Fig. S2B).

Cloning, purification, and characterization of Hpo, Nfo, Ami, and Iso. These enzymes were colorless, indicating that no tightly associated chromophores were present.

Hpo—The *hpo* gene was cloned from the gene cluster and over-expressed in *E. coli* BL21(DE3). Hpo was purified and showed an apparent molecular mass of 40 kDa which corresponds to the predicted gene product weight (Fig. 2A). The effect of pH on the spectrophotometric assay is shown in Fig. 2B. Optimum pH was 6.5 in phosphate buffer. The optimum temperature for the enzymatic reaction was approximately 20°C and was identified by measuring the initial reaction velocity for 1 min (Fig. 2C). Among the 10 metal salts tested, only Fe^{2+} (0.025 mM) showed markedly increased enzyme activity (Fig. 2D). The double reciprocal plots of initial velocity against DHP concentration were straight lines, indicating that Michaelis-Menten saturation kinetics were characteristic of the substrate. The calculated apparent K_m for DHP was 0.168 μM, V_{max} was

7.0 U mg^{-1}, and k_{cat} was 11.0 s^{-1}. The product of the enzymatic reaction, *N*-formylmaleamate (NFM), was also detected by the API 4000 liquid chromatography-mass spectrometry (LC-MS) system (Applied Biosystems, Foster City, CA). A molecular ion at an m/z value of 112.2 corresponds to DHP according to positive mass spectrometry. Additionally, negative mass spectrometry experiments revealed an $(M-H)^-$ peak at m/z 142.1, corresponding to NFM, which is in agreement with that reported by Jimenez[18] (Fig. S3).

Nfo, Ami, and Iso—The 29 kDa protein Nfo is consistent with the predicted product of the *nfo* gene (Fig. 3A). Because NFM was not commercially available, it was chemically synthesized, and the product was confirmed by ^1H nuclear magnetic resonance (NMR) (Fig. S4). The signals were assigned to the corresponding protons as indicated in the box (Fig. S4). Nfo activity was measured through its production of formate by a coupled reaction with nicotinamide adenine dinucleotide (NAD)-dependent formate dehydrogenase (Fdh) (Fig. 3B). Purified Ami (Fig. 3A) transformed maleamic acid to maleic acid with the production of NH_4^+ (not shown). NH_4^+ concentration was monitored by a decrease in the amount of nicotinamide adenine dinucleotide phosphate (NADPH) measured at 340 nm in a reaction buffer containing glutamate dehydrogenase (Gdh) (Fig. 3C). Iso was also expressed in *E. coli* BL21(DE3)/ pET28a-*iso*, and the 28-kDa enzyme was purified (Fig. 3D). Iso is similar to an isomerase from *Ralstonia eutropha* H16 (71% amino acid sequence homology), and to the Asp/Glu racemase of *Serratia proteamaculans* 568 (72% amino acid sequence homology). Iso
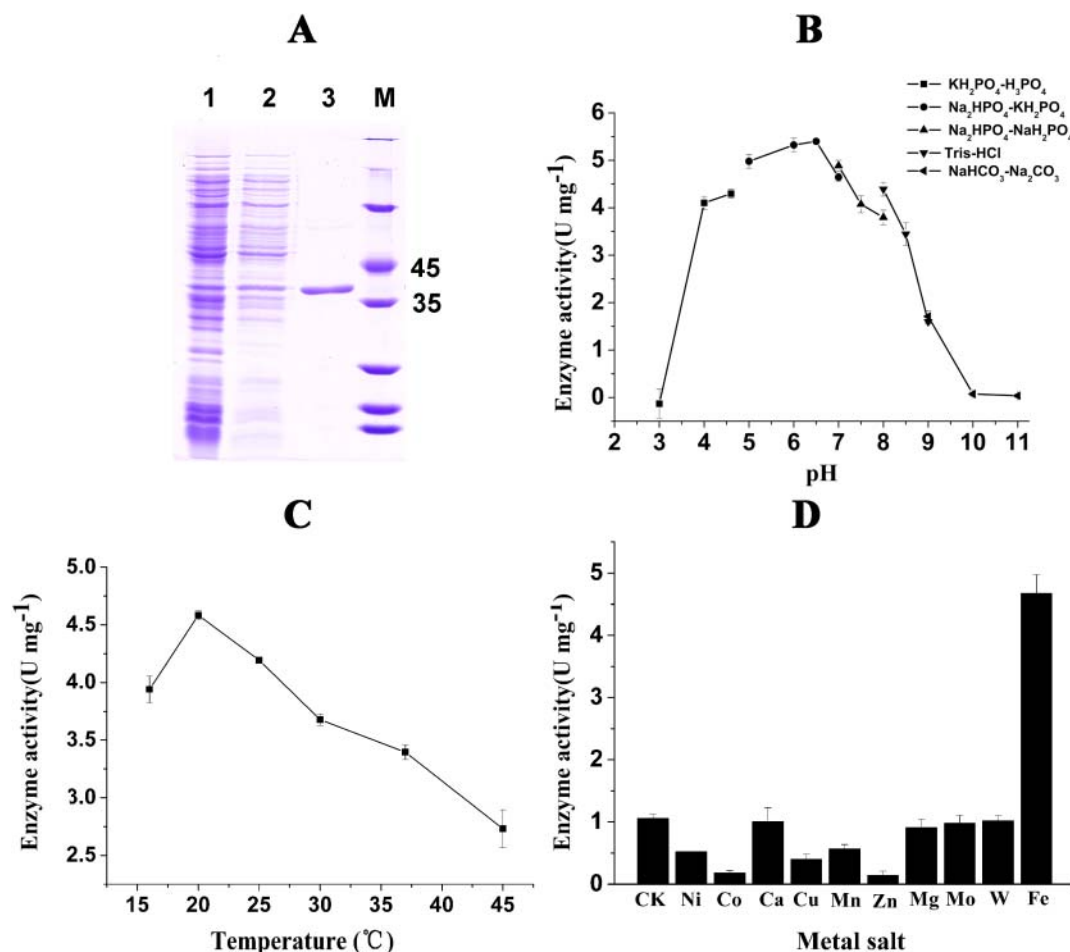

Figure 2 | Characterization of Hpo. (A) SDS-PAGE. M, molecular size markers; lanes 1 and 2, cell extracts of expressed Hpo in *E. coli* BL21(DE3) expressing His_6-Hpo; lane 3, purified His_6-Hpo. (B) pH dependence of Hpo specific activity. (C) Effect of varying temperatures on specific Hpo activity. (D) Effect of the various metal salts on Hpo specific activity. CK, without metal salt; Ni, Ni^{2+}; Co, Co^{2+}; Ca, Ca^{2+}; Cu, Cu^{2+}; Mn, Mn^{2+}; Zn, Zn^{2+}; Mg, Mg^{2+}; Mo, MoO_4^{2-}; W, WO_4^{2-}; Fe, Fe^{2+}.
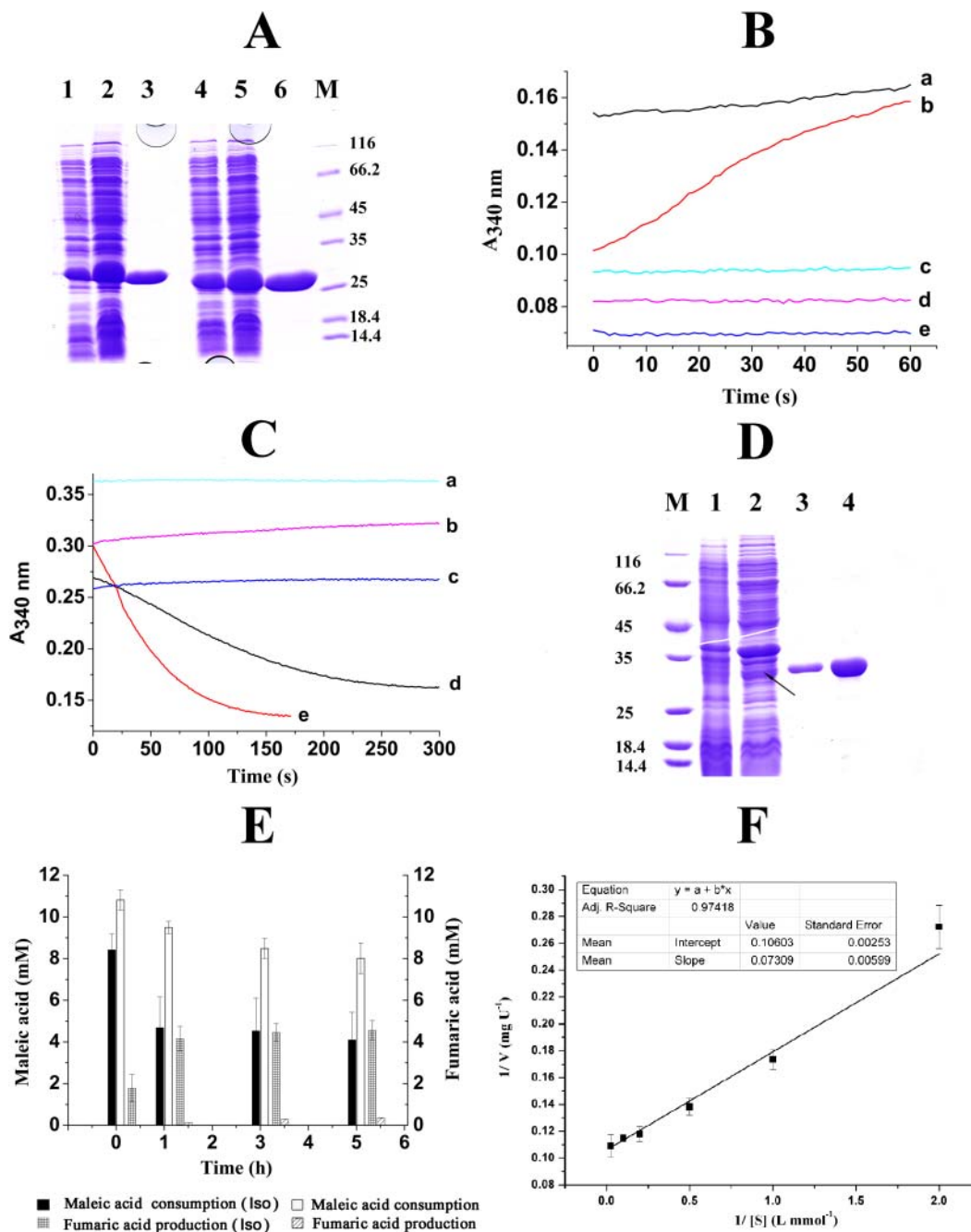
Figure 3 | Characterization of Nfo, Ami, and Iso. (A) SDS-PAGE of Nfo and Ami. M, molecular size markers; lanes 1 and 2, cell extracts of *E. coli* BL21(DE3) expressing His$_6$-Nfo; lane 3, purified His$_6$-Nfo; lanes 4 and 5, cell extracts of *E. coli* BL21(DE3) expressing His$_6$-Ami; 6, purified His$_6$-Ami. (B) Nfo activity, *a*, complete reaction: 695 µl buffer + 5 µl NAD + 50 µl Fdh + 50 µl Nfo + 200 µl NFM; *b*, positive control containing HCOOH (1.65 mM) instead of Nfo and NFM; *c*, negative control without NFM; *d*, negative control without Nfo; *e*, negative control without Nfo and NAD. (C) Enzymatic activity of Ami, *a*, negative control without Ami; *b*, negative control, without maleamic acid and Ami; *c*, negative control without maleamic acid; *d*, complete reaction containing 480 µl buffer (50 mM Tris-HCl + 0.001 mol l^{-1} EDTA), 200 µl maleamic acid (0.034 mol l^{-1}), 10 µl α-ketoglutaric acid (0.5 mol l^{-1}), 10 µl NADPH (0.01 mol l^{-1}), 100 µl Gdh (9.5 unit ml^{-1}), and 200 µl amidase (0.106 mg protein ml^{-1}); *e*, positive control, containing ammonia (30 µM NH$_4$Cl) instead of maleamic acid and Ami. (D) SDS-PAGE of Iso. M, molecular size markers; lanes 1 and 2, cell extracts of expressed Iso in *E. coli* BL21(DE3); lanes 3 and 4, purified His$_6$-tagged Iso. (E) Transformation of maleic acid by Iso. (F) Determination of K_m of Iso.

activity was determined by high-performance liquid chromatography (HPLC) (Agilent 1200 series, Hewlett-Packard Corp., Santa Clara, CA, USA) analysis in the presence of a mercaptan. Purified Iso catalyzed the isomerization of maleate acid to fumaric acid (Fig. 3E). The apparent K_m value of Iso was determined spectrophotometrically, monitoring maleate acid consumption at 290 nm. The assay was performed at 30°C in 50 mM Tris-HCl buffer (pH 8.4). The

calculated apparent K_m for maleate acid was 0.689 mM, V_{max} was 9.4 U mg^{-1} proteins, and k_{cat} was 4.0 s^{-1} (Fig. 3F), respectively.

Deletion of the hpo gene. The *hpo* gene was deleted separately, and the related cell growth and resting cell reactions were all performed. The *hpo* gene deletion mutant could grow in nicotine medium and turn its color to saddle brown, whereas the color culture medium of

the wild type strain S16 changed into pale green (Fig. 4A). Cells of *hpo* gene deletion mutant and wild type strain S16 were harvested in the mid-growth phase by centrifugation at 5,000 × *g* for 10 min at 4°C, washed three times with 0.02 M Tris-HCl buffer (pH 7) and suspended in the same buffer at $OD_{600\ nm}$ (called resting cells) value of 7. Resting cells of both cell types have the ability to transform nicotine (Fig. 4B). However, resting cells of *hpo* gene deletion mutant could not degrade DHP, different from the wild-type strain S16 (Fig. 4C). These results demonstrate that enzyme Hpo is crucial for DHP transformation and nicotine degradation by the strain.

Comparative genome analysis. Comparative genome analysis was performed using Mauve[20], and genomic islands (GIs) were analyzed using the IslandViewer software[21]. Phylogenetic tree construction using MEGA 4.1[22] (containing genes *hpo*, *nfo*, *ami* and *iso*, Fig. 5A) showed that the gene cluster from S16 is most closely
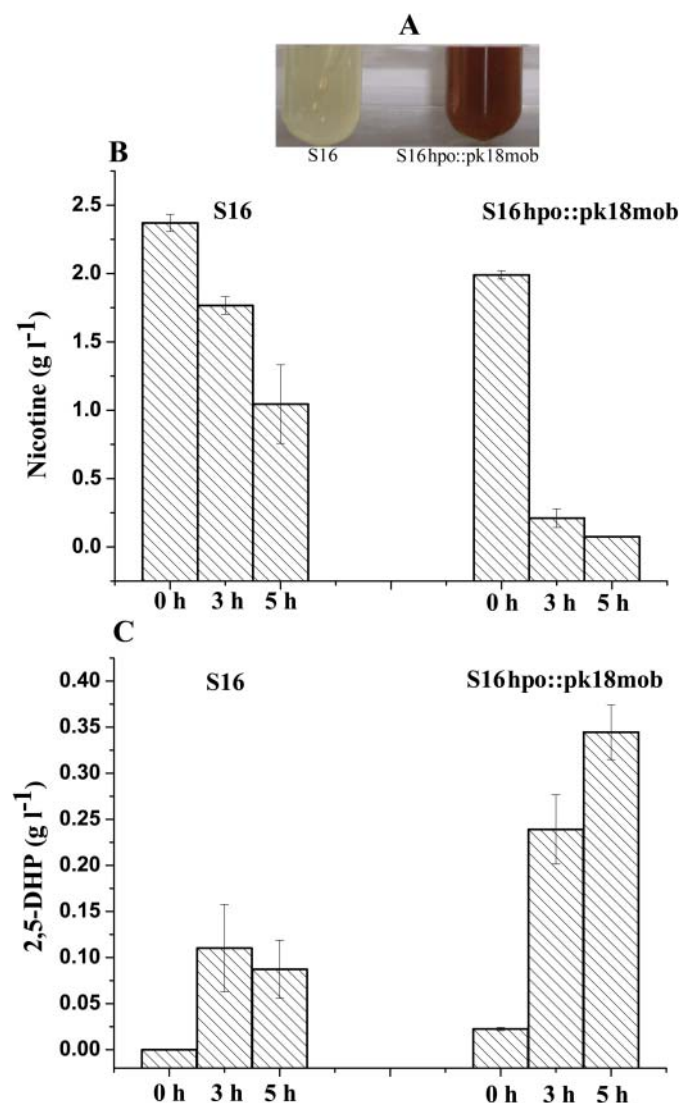
related to *Octadecabacter antarcticus* 238. The phylogenetic trees constructed with the neighbor joining (NJ) method for the individual proteins further refined the analysis, identifying similarities among these proteins (Fig. 5B). Hpo of *P. putida* S16 is closest to the ortholog from *Rhizobium* WSM1325, whereas Nfo and Ami are closest to *O. antarcticus* 238. Iso of *P. putida* S16 is in a deep branch of its own. Moreover, 29 GIs were identified in the complete genome of strain S16. The *nic*2 gene cluster is located within the largest GI (43,989 bp in length), which has a G+C content of 52.4% and codes for 8 transposases[16] (Fig. S1). The GI containing the late pathway genes was not found in any of the 5 completely sequenced genome strains of *P. putida* namely *P. putida* KT2440, W619, F1, GB-1 and BIRD-1. The nicotinic acid degrading genes *nicAB* of *P. putida* KT2440[18] were found in the genomes of 4 other *P. putida* strains. However, the *nicAB* genes were not found in the strain S16 genome. Attempts to degrade nicotinic acid by resting cells of strain S16 did not result in any degradation after 24 h of incubation (data not shown).

Discussion

The analysis of genes and the biochemical characterization of nicotine catabolism enzymes serve as bases for rationally improving *Pseudomonas* strains for nicotine waste disposal[2,4,23]. The characterization of genes and gene products involved in nicotine degradation in *Pseudomonas* can lead to a full understanding of this catabolic activity. The identification of genes involved in the nicotine degradation pathway increases the possibility to clone related genes from other organisms, including noncultivable environmental samples. 6-Hydroxy-3-succinoylpyridine (HSP) and 2,5-dihydroxy-pyridine (DHP) in nicotine degradation are useful precursors for chemical synthesis[10,13]. Knowledge of nicotine degradation genes such as *hpo* and *hspB*[15] can be adapted in detoxification programs for tobacco wastes and synthesis of useful products of pharmaceutical importance. These genes may also be useful for the modification or degradation of alkaloid substances and other heterocyclic aromatic compounds.

The complete proposed nicotine degradation pathway is presented in Fig. 1A. The discovered *nic*2 gene cluster encodes for 5 enzymes that convert HSP to fumaric acid, formic acid, and ammonia (Fig. 1A). All of the enzymes were cloned and expressed in *E. coli*, and their biochemical activities were confirmed. The *nic*2 gene cluster is separated by more than 30 kb of DNA from the *nic*1 gene cluster, which contains *nicA* and *hspA*[13–16].

Several gene clusters in other microorganisms with similarity to *nic*2 in *P. putida* S16 were found in the databases (Fig. 1B). No reports on nicotine degradation in these strains have been published, except for strain S16. Gene sequence alignment showed that the 4 enzymes (Hpo, Nfo, Ami, and Iso) showed variations (36%–69% amino acid homology), from their closest homologues in *P. putida* KT2440, which were not reported to degrade nicotine. The cluster (*iso-ami* part) shows a low level of homology to the partly syntenic gene clusters of other *P. putida* strains, KT2440, F1, GB-1, and W619, which encodes proteins of only 33%–72% amino acid homology (Fig. 1B). However, these strains may degrade nicotinic acid instead of nicotine and are very similar to each other (mostly > 95% amino acid homology, Fig. S5). The gene cluster that is highly similar to the cluster (*iso-ami* part) of *P. putida* S16 was from *O. antarcticus* 238, which has not been reported to be involved in nicotine or nicotinic acid degradation. The genes are syntenic and the corresponding proteins are 60%–81% homologous (Fig. 1B). The GC content of the 3,233-bp gene cluster (*iso-ami* part) is 48%. The genome of strain S16 consists of a single circular chromosome 5,984,790 bp in length, with a GC content of 62.3%, and do not contain any plasmids[16]. In contrast, the GC contents of the *nic* clusters of the other *P. putida* strains are all approximately 64%. The relatively low GC content of the S16-*nic*2 gene cluster and the divergence of the amino acid

Figure 4 | Nicotine transformation by *P. putida* S16 and *P. putida* S16 hpo::pk18mob. (A) The liquid culture of *P. putida* S16 and *P. putida* S16 hpo::pk18mob in nicotine medium. The medium was cultured at 30°C for 16 h. (B) The concentration of nicotine in *P. putida* S16 and *P. putida* S16 hpo::pk18mob resting cell systems. The resting cell systems were cultured at 30°C; sampling was conducted at 0, 3 and 5 h. (C) The concentration of 2,5-DHP in *P. putida* S16 and *P. putida* S16 hpo::pk18mob resting cell systems. The resting cell systems were cultured at 30°C sampling was conducted at 0, 3 and 5 h.
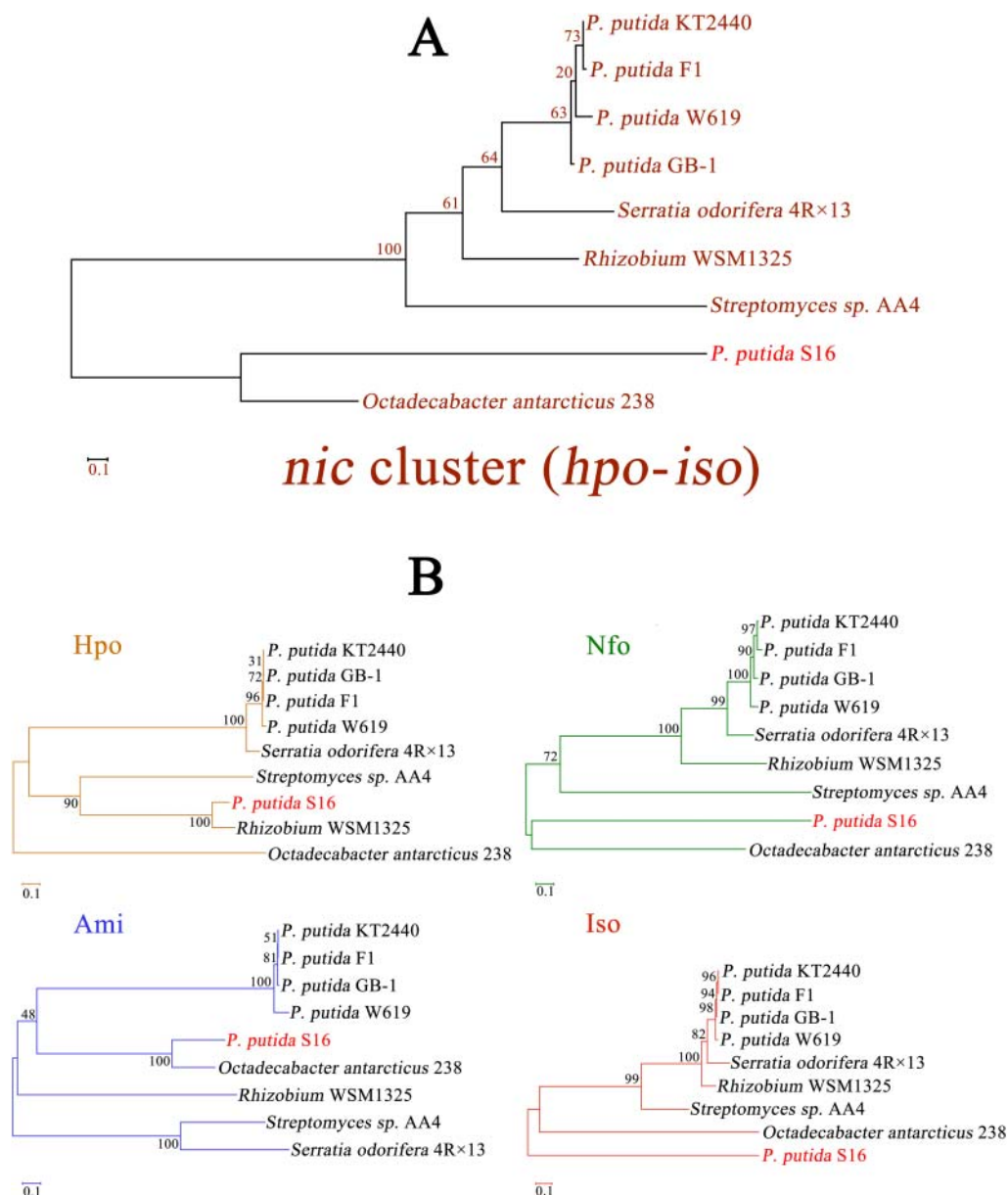
Figure 5 | Phylogenetic trees of the *nic* gene cluster and 4 related enzymes in late pathway of nicotine degradation. The phylogenetic trees were constructed with the neighbor joining method (NJ). (A) Phylogenetic tree of *nic* clusters of different strains constructed using MEGA 4.1. (B) Phylogenetic trees of Hpo, Nfo, Ami, and Iso of different strains constructed using MEGA 4.1.

sequences in Fig. 5 suggested that *nic*2 of *P. putida* S16 may have originated from a genus other than *Pseudomonas*.

Nicotinic acid degradation pathways have been characterized in several microorganisms such as *Pseudomonas*, *Bacillus*, and *Eubacterium* [17,18,24–28]. Behrman and Stanier reported that nicotinic acid metabolism in *Pseudomonas* proceeds through the maleamate pathway, involving DHP, maleamate, maleate, and fumarate as intermediates[25]. This is similar to the late pathway of nicotine degradation in strain S16. No ortholog of NicAB, the two-component nicotinic acid hydroxylase of *P. putida* KT2440[18], was found in the *P. putida* S16 genomic sequence, suggesting the inability of strain S16 to catabolize nicotinic acid.

The nicotine degradation genes may be useful for the genetic engineering of nicotine catabolism and for the production of specialist enzymes. The proposed reactions catalyzed by the 4 enzymes, 2,5-DHP dioxygenase (Hpo, EC 1.13.11.9), *N*-formylmaleamate deformylase (Nfo, EC 3.5.1.106), maleamate amidase (Ami, EC 3.5.1.107), and maleate *cis-trans* isomerase (Iso, EC 5.2.1.1), are particularly

interesting. One of the key enzymes involved in nicotine degradation is the 2,5-DHP-oxidase (Hpo), which requires a ferrous ion for activation. Similar properties were observed in other dioxygenases that catalyze the cleavage of the aromatic ring[18]. This study proposes that the sensitivity to oxidizing agents is at least partially related to the weak binding of the catalytically active Fe^{2+} ion to Hpo. Hpo of *P. putida* S16 did not require an external reduced cofactor and contained no flavin or heme group. The Hpo enzymes (Fig. 1, orange arrows) from strain S16 and *P. putida* KT2440 catalyze the similar enzymatic reactions, although their protein sequences are only 43% homologous. Orthologs of Nfo, Ami, and Iso from the nicotine degradation pathway were also characterized in this study. Both Nfo (deformylase) and Ami (amidase) belong to the hydrolase family, which act on carbon-nitrogen bonds of linear amides[18,29]. Nfo catalyzes the deformylation of NFM to release maleamic and formic acid[30], whereas Ami catalyzes the hydrolysis of an amide[29]. Iso (maleate *cis-trans* isomerase) has orthologs in several maleate-assimilating bacteria and was shown to reversibly convert maleate to

Table 1 | Primers

Primer	Sequence (5'-3')	Recombinant plasmid
Hpo (*hpo*)	5'aata<u>ccatgg</u>ca**atggaccatgtgagttttaccg**3'	pET28a-*hpo*
	5' aaac<u>ctcgag</u>**cctttgcactagctgaatttcttt**3'	
Nfo (*nfo*)	5'aat<u>ccatgg</u>ca**atgaaagggtacaacgtttatgcaaa**3'	pET28a-*nfo*
	5'aaac<u>ctcgag</u>**tcgattgctgactgcagttatgaagcctt**3'	
Ami (*ami*)	5'ccca<u>ccatgg</u>ca**atgtcacaaaaagaagtatatgac**3'	pET28a-*ami*
	5'aaat<u>ctcgag</u>**gcccgcaaccgatcgcagccattttaa**3'	
Iso (*iso*)	5'aatc<u>ccatgg</u>caa**tggaagctatgaaggttgtacgcgtt**3'	pET28a-*iso*
	5'aacc<u>ctcgag</u>**gtaggcacctgaaagaagagttccacc**3'	

Bold front, the native gene sequence; <u>ccatgg</u>, NcoI site; <u>ctcgag</u>, XhoI site.

fumarate. Maleate *cis-trans* isomerases have received considerable research attention owing to its potential to serve as industrial catalysts, because fumarate is a substrate for aspartic acid formation[31].

In summary, a gene cluster encoding the nicotine catabolic enzymes of the late steps in the nicotine degradation was discovered and biochemically characterized. Genomic analysis of strain S16 revealed that genes located in the largest genome island are crucial for nicotine degradation. This study has also identified genes that may be useful for the genetic engineering of nicotine catabolism and for the production of specialist enzymes.

Methods

Bacterial strains and growth conditions. *E. coli* BL21(DE3) was employed as a host for both plasmids and the expression strain, cultured in Lysogeny broth medium and maintained at 37°C. *P. putida* S16 was grown in Nic medium and incubated at 30°C[9].

Chemicals and biochemicals. Fdh, Gdh, formate, α-ketoglutaric acid, maleamic acid, maleic acid, fumaric acid, dithiothreitol, NADPH, and NAD, were obtained from Sigma-Aldrich (St. Louis, MO, USA). L-(-)-Nicotine (≥ 99% purity) was obtained from Fluka Chemie GmbH (Buchs Corp., Buchs, Switzerland).

NFM synthesis. The product was prepared as reported elsewhere with minor modifications[27]. Maleic anhydride (10 g) was heated to 80°C under a nitrogen atmosphere in a 250-ml round bottom flask equipped with a reflux condenser. Anhydrous formamide was added (10 ml), and the reaction mixture was stirred slowly with a magnetic stirrer for 10 h at 80°C. The product was analyzed by NMR spectroscopy.

Identification of genes in the late steps. A fragment containing the gene cluster involved in the late steps of nicotine degradation was identified through data mining for amino acid sequences of NicX, NicD, NicF, and NicE of *P. putida* KT2440[18] with the genome sequence of *P. putida* S16[16]. Each gene in the fragment was subcloned into pET28a and functionally analyzed. DNA manipulation and transformation were performed according to standard procedures[32]. The primers employed in this study are listed in Table 1. Primers were designed to incorporate an NcoI site in the forward primer and an XhoI site in the reverse primer. The DNA fragments bearing *hpo*, *nfo*, *ami*, and *iso* were amplified from genomic DNA using *pfu* polymerase (Tiangen, China) digested with NcoI and XhoI, and ligated into the NcoI-XhoI sites of pET28a. The resulting plasmids were used to transform *E. coli* BL21(DE3). Cells harboring the recombinant plasmids were cultured in LB medium containing 100 mg liter⁻¹ kanamycin and maintained at 37°C until the OD$_{600}$ reading reached 0.6. IPTG was then added to a final concentration of 1 mM and the cultures were incubated for another 6 h at 30°C to express the proteins. His$_6$-tagged Hpo, Nfo, Ami, and Iso were purified using a column of Ni-NTA agarose (Qiagen).

Enzyme activities of Hpo, Nfo, Ami and Iso. Hpo activity was measured at 20°C using a UV-Vis 2550 spectrophotometer (Shimadzu) at 320 nm ($\varepsilon_{320} = 5200$ cm⁻¹ M⁻¹) as the previously reported[17,18]. The reaction mixture contained 0.02 mg ml⁻¹ DHP, 0.025 mM Fe²⁺, 18.2 mM Tris-HCl buffer (pH 8.0), and 0.0125 mg protein ml⁻¹ enzyme in a total volume of 1 ml. One unit of activity was defined as the amount of enzyme that catalyzed the disappearance of 1 μmol of substrate in 1 min.

Nfo and Ami activities were measured at 20°C, using the UV-Vis 2550 spectrophotometer at 340 nm. The Nfo assay mixture contained 695 μl Tris-HCl buffer (50 mM, pH 8.0), 5 μl NAD (0.33 M), 50 μl Fdh (9.2 unit ml⁻¹), 200 μl NFM (286 μmol l⁻¹), and 50 μl Nfo (0.57 mg protein ml⁻¹). The Ami assay mixture contained 480 μl buffer (50 mM Tris-HCl + 0.001 mol l⁻¹ EDTA), 200 μl maleamic acid (0.034 mol l⁻¹), 10 μl α-ketoglutaric acid (0.5 mol l⁻¹), 10 μl NADPH (0.01 mol l⁻¹), 100 μl Gdh (9.5 unit ml⁻¹), and 200 μl Ami (0.11 mg protein ml⁻¹).

Iso activity was measured at 30°C, using the UV-Vis 2550 spectrophotometer at 290 nm as previously reported[31]. The Iso assay mixture contained 50 mM Tris-Cl (pH 8.4), 10 μl 1-thioglycerol (500 mM), an appropriate volume of maleate (1 M, pH 7), and 5 μl isomerase (10.1 mg protein ml⁻¹) in a total volume of 1 ml.

Analytical techniques. DHP, NFM, maleamic acid, and maleic acid were detected by HPLC and confirmed by direct-insertion mass spectra recorded on the API 4000 LC-MS system. MS analysis was performed in both negative and positive-ion turbo ion spray ionization mode.

Nonquantitative RT-PCR. RT-PCR procedure was followed as previously reported[14]. Total RNA was isolated from *P. putida* S16 by using a Total RNA kit I (Omega, USA). Contaminating DNA was treated with DNase I (RNAse-free; Fermentas, EU) at 1 U per 1 μg of total RNA for 30 min at 37°C. RT-PCR was performed in 50-μl reaction mixtures containing approximately 400 ng of total RNA and 20 pmol of each primer with a Prime Script™ one step RT-PCR kit (Takara, Japan). The amplification conditions employed for RT-PCR was as follows: 50°C for 30 min; 94°C for 2 min; 30 cycles of 94°C for 30 s; 57°C for *hpo*, *nfo*, and *ami*, 68°C for *iso*, and 72°C for 2 min. The primers employed in the amplification are listed in Table 1. RNA was used as a negative control to confirm the absence of DNA that may be contaminating the RNA preparations.

P. putida S16 mutant (*hpo* gene deletion). To delete the *hpo* gene in strain S16 by single homologous recombination, internal fragments were amplified by PCR and cloned into the polylinker region of pK18mob (*hpo* -347-f: <u>CAGTGAATTCAACCTCCTGAGCTTCTGGCCC</u>; *hpo* -708-r: <u>CTTAGTCGACTTCAAGACCGCCGCGAATATC</u>). The pK18mob-*hpo* was transformed and the deletion mutant was screened as previously described[15].

Nucleotide sequence accession number. The nucleotide sequence reported in the present study has been deposited in GenBank under accession number GQ857548.

1. Novotny, T. E. & Zhao, F. Consumption and production waste: another externality of tobacco use. *Tob. Control* **8**, 75–80 (1999).
2. Brandsch, R. Microbiology and biochemistry of nicotine degradation. *Appl. Microbiol. Biotechnol.* **69**, 493–498 (2006).
3. Eberhardt, H. The Biological degradation of nicotine by nicotinophilic microorganisms. *Beitr. Tabakforsch. Int.* **16**, 119–129 (1995).
4. Li, H. J., Li, X. M., Duan, Y. Q., Zhang, K. Q. & Yang, J. K. Biotransformation of nicotine by microbiology: the case of *Pseudomonas* spp. *Appl. Microbiol. Biotechnol.* **86**, 11–17 (2010).
5. Ruan, A. D., Min, H., Peng, X. H. & Huang, Z. Isolation and characterization of *Pseudomonas* sp. strain HF-1, capable of degrading nicotine. *Res. Microbiol.* **156**, 700–706 (2005).
6. Wada, E. & Yamasaki, K. Mechanism of microbial degradation of nicotine. *Science* **117**, 152–153 (1953).
7. Wada, E. Microbial degradation of the tobacco alkaloids, and some related compounds. *Arch. Biochem. Biophys.* **72**, 145–162 (1957).
8. Wang, M. Z., Yang, C. Q., Min, H., Lv, Z. M. & Jia, X. Y. Bioaugmentation with the nicotine-degrading bacterium *Pseudomonas* sp. HF-1 in a sequencing batch reactor treating tobacco wastewater: Degradation study and analysis of its mechanisms. *Water Res.* **43**, 4187–4196 (2009).
9. Wang, S. N. *et al.* Biodegradation and detoxification of nicotine in tobacco solid waste by a *Pseudomonas* sp. *Biotechnol. Lett.* **26**, 1493–1496 (2004).
10. Wang, S. N., Xu, P., Tang, H. Z., Meng, J., Liu, X. L. & Ma, C. Q. 'Green' route to 6-hydroxy-3-succinoyl-pyridine from (S)-nicotine of tobacco waste by whole cells of a *Pseudomonas* sp. *Environ. Sci. Technol.* **39**, 6877–6880 (2005).
11. Zhong, W. H. *et al.* Degradation of nicotine in tobacco waste extract by newly isolated *Pseudomonas* sp. ZUTSKD. *Bioresource Technol.* **101**, 6935–6941 (2010).
12. Wang, S. N., Liu, Z., Tang, H. Z., Meng, J. & Xu, P. Characterization of environmentally friendly nicotine degradation by *Pseudomonas putida* biotype a strain S16. *Microbiology-SGM* **153**, 1556–1565 (2007).
13. Tang, H. Z. *et al.* A novel gene, encoding 6-hydroxy-3-succinoylpyridine hydroxylase, involved in nicotine degradation by *Pseudomonas putida* strain S16. *Appl. Environ. Microbiol.* **74**, 1567–1574 (2008).
14. Tang, H. Z. *et al.* Novel nicotine oxidoreductase-encoding gene involved in nicotine degradation by *Pseudomonas putida* strain S16. *Appl. Environ. Microbiol.* **75**, 772–778 (2009).

15. Tang, H. Z. *et al.* A Novel NADH-dependent and FAD-containing hydroxylase is crucial for nicotine degradation by *Pseudomonas putida*. *J. Biol. Chem.* **286**, 39179–39187 (2011).

16. Yu, H. *et al.* Complete genome sequence of nicotine-degrading *Pseudomonas putida* strain S16. *J. Bacteriol.* **193**, 5541–5542 (2011).

17. Gauthier, J. J. & Rittenberg, S. C. The metabolism of nicotinic acid. I. Purification and properties of 2, 5-dihydroxypyridine oxygenase from *Pseudomonas putida* N-9. *J. Biol. Chem.* **246**, 3737–3742 (1971a).

18. Jimenez, J. I. *et al.* Deciphering the genetic determinants for aerobic nicotinic acid degradation: The *nic* cluster from *Pseudomonas putida* KT2440. *Proc. Natl. Acad. Sci. USA* **105**, 11329–11334 (2008).

19. Shine, J. & Dalgarno, L. Determinant of cistron specificity in bacterial ribosomes. *Nature* **254**, 34–38 (1975).

20. Darling, A. C., Mau, B., Blattner, F. R. & Perna, N. T. Mauve:multiple alignment of conserved genomic sequence with rearrangements. *Genome Res.* **14**, 1394–1403 (2004).

21. Langille, M. G. & Brinkman, F. S. IslandViewer: an integrated interface for computational identification and visualization of genomic islands. *Bioinformatics* **25**, 664–665 (2009).

22. Kumar, S., Nei, M., Dudley, J. & Tamura, K. MEGA: a biologist-centric software for evolutionary analysis of DNA and protein sequences. *Brief Bioinform.* **9**, 299–306 (2008).

23. Civilini, M., Domenis, C., Sebastianutto, N. & Bertoldi, Md. Nicotine decontamination of tobacco agro-industrial waste and its degradation by micro-organisms. *Waste Manage. Res.* **15**, 349–358 (1997).

24. Alhapel, A. *et al.* Molecular and functional analysis of nicotinate catabolism in *Eubacterium barkeri*. *Proc. Natl. Acad. Sci. USA* **103**, 12341–12346 (2006).

25. Behrman, E. J. & Stanier, R. Y. The bacterial oxidation of nicotinic acid. *J. Biol. Chem.* **228**, 923–945 (1957).

26. Ensign, J. C. & Rittenberg, S. C. The pathway of nicotinic acid oxidation by a *Bacillus* species. *J. Biol. Chem.* **239**, 2285–2291 (1964).

27. Gauthier, J. J. & Rittenberg, S. C. The metabolism of nicotinic acid. II. 2, 5-dihydroxypyridine oxidation, product formation, and oxygen 18 incorporation. *J. Biol. Chem.* **246**, 3743–3748 (1971b).

28. Nakano, H. *et al.* Purification, characterization and gene cloning of 6-hydroxynicotinate 3-monooxygenase from *Pseudomonas fluorescens* TN5. *Eur. J. Biochem.* **260**, 120–126 (1999).

29. Bray, H. G., James, S. P., Raffan, I. M., Ryman, B. E. & Thorpe, W. V. The fate of certain organic acids and amides in the rabbit. 7. An amidase of rabbit liver. *Biochem. J.* **44**, 618–625 (1949).

30. Mazel, D., Pochet, S. & Marliere, P. Genetic characterization of polypeptide deformylase, a distinctive enzyme of eubacterial translation. *EMBO. J.* **13**, 914–923 (1994).

31. Scher, W. & Jakoby, W. B. Maleate isomerase. *J. Biol. Chem.* **244**, 1878-1882 (1969).

32. Sambrook, J. & Russell, D. W. Molecular cloning: A laboratory manual, 3ʳᵈ ed. Cold Spring Harbor Laboratory (2001).

Acknowledgements

Author contributions

P.X. and H.T. conceived and designed the project and experiments. H.T., Y.Y., L.W., H.Y., and Y.R. performed the experiments. P.X. and G.W. analyzed the data. H.T. and P.X. wrote the paper.

Additional information

Supplementary information accompanies this paper at http://www.nature.com/scientificreports

Competing financial interests: The authors declare no competing financial interests.

How to cite this article: Tang, H. *et al.* Genomic analysis of *Pseudomonas putida*: genes in a genome island are crucial for nicotine degradation. *Sci. Rep.* **2**, 377; DOI:10.1038/srep00377 (2012).